# Dynamic Band Imaging:
# Image Enhancement for Endoscopic Diagnosis


Toshiya Nakaguchi[*] *nakaguchi@faculty.chiba-u.jp*
Atsunori Sakama[**] *sa1125@graduate.chiba-u.jp*
Satoki Zenbutsu[***] *zenbutsu@office.chiba-u.jp*
Norimichi Tsumura[*] *tsumura@faculty.chiba-u.jp*
Yoichi Miyake[*,***] *miyake@faculty.chiba-u.jp*

[*]*Graduate School of Advanced Integration Science, Chiba University*
*1-33, Yayoi-cho, Inage-ku, Chiba, 263-8522, Japan*
[**]*Department of Optical Medicine, Chiba University Hospital*
*1-8-1, Inohana, Chuo-ku, Chiba, 260-8677, Japan*
[***]*Research Center for Frontier Medical Engineering, Chiba University*
*1-33, Yayoi-cho, Inage-ku, Chiba, 263-8522, Japan*

Correspondence: Toshiya Nakaguchi, Ph.D
Graduate School of Advanced Integration Science
Chiba University
1-33, Yayoi-cho, Inage-ku, Chiba, 263-8522, Japan
Phone/Fax: +81-43-290-3296
Email: nakaguchi@faculty.chiba-u.jp

**Abstract**

In this study we propose an endoscopic image enhancement technique named dynamic band imaging (DBI) which temporally changes color conversion matrix. DBI is based on the estimation of multi-spectral band images to enhance the endoscopic color images in order to distinguish the slight color difference of early-stage cancer more clearly. Since this method can be implemented by only using software approach, it is easy to upgrade the devices whereas narrow band technique requires hardware upgrading. From the results of fundamental analysis by subjective evaluations, DBI represents the effectiveness for image enhancement in comparison with the typical still image evaluation. Besides we have developed a user interface to determine six parameters of this method easily. By using this device, appropriate parameters for practical endoscopic diagnosis have been obtained. DBI is found as the new effective method to enhance color endoscopic images.

Keywords: Color enhancement of Endoscopy, Spectral image processing, Real-time processing, Visual characteristics

## 1. Introduction

Since color images taken by electronic endoscopes provide important information for diagnosis of various kinds of digestive diseases, it is important to observe the fine structure of the mucous membrane wall in detail. Color reproduction of electronic endoscopes, however, is not enough to diagnose the early stage of the diagnosis. Therefore, it has been required to improve color reproduction of electronic endoscopes in order to distinguish the slight color difference of early-stage cancer more clearly [1].

Toward such purpose, several methods have been proposed in the past. Based on the report that index of hemoglobin (IHb) correlates well with mucosal microcirculation, the adapted IHb color enhancement system has been developed [2]. Because this method can be implemented by real-time software approach, it is widely used in the market of commercial endoscopes. Although the efficacy of this technique for the digestive systems has been reported [3, 4], its disadvantage has been also reported, that it would increase the number of false positives of the non-polypoid lesions [5]. Autofluorescence endoscopy exploits either autofluorescence characteristics of naturally-occurring molecules in the tissue or fluorescence caused by an exogenously administered fluorescent drug [6-8]. By using this technique, the detection of abnormal lesions depends on changes in the concentration or depth distribution of the endogenous fluorophores that can affect the fluorescence intensity or spectrum. In 2002, Gono et al. have proposed the narrow band imaging (NBI) technique [9-11] to improve the image quality with regard to such fine structure by adjusting the spectrum feature in consideration of the wavelength dependence of the light penetration depth into the tissue. This method is quite significant and is remarkably focused on by medical doctors [12, 13]. However because the NBI and autofluorescence endoscopy require dedicated hardware, their costs are very high and they can not perform the optimal analysis for arbitral diseases because of the fixed wavelength.

To overcome such problems, Miyake et al. have proposed the image enhancement technique using the multi-spectral images in 2005 [14], which is based on the spectral analysis as follows. In 1988, they have first developed the endoscope spectrophotometer [15] to measure the spectral reflectance of gastric mucous membrane directly and precisely. Many measured spectra of the gastric and rectal mucous membrane have been analyzed by principal component analysis and they showed that the reflectance spectra can adequately be described by only three principal components. Based on this experimental result, it was shown that the reflectance spectra of gastric and rectal mucous membrane can be estimated from the R, G, and B signals of the conventional electronic endoscopes. In the study of [14], three of estimated single band images were chosen from estimated multi-band images and were assigned to RGB channels again. Although some endoscopic images are improved effectively by using this method, since it is essentially only a simple color conversion by using a $3\times3$ matrix, it has the limitation of enhancement.

Therefore in this study we propose a new image enhancement technique based on estimated multi-spectral imaging named dynamic band imaging (DBI). Human perception has more sensitivity against the changing stimulus than the static stimulus. In order to distinguish the slight color difference, it can be thought that color-enhanced movies are more effective than still images. DBI is an extension of Miyake's synthesizing method and exploits temporal change of color conversion matrix based on the above hypothesis. Since DBI can be implemented by only using software post-processing, it is very easy to realize into conventional endoscopes additionally whereas conventional color-enhancement techniques require hardware upgrading. In this study, we first examine the fundamental effectiveness of DBI by performing subjective experiments and the results are analyzed by employing logistic regression analysis. Actually DBI has a lot of parameters and its change can be designed freely. Hence in this study we focus on six example cases to confirm the basic efficacy of the temporal parameter change and evaluate these cases by using logistic regression analysis. Besides we implement DBI for the practical medical application for the endoscopic diagnosis. Because DBI has many parameters which need to change simultaneously, it is very difficult task to find the best changing way of parameters by using conventional user interface. Therefore we have developed an interface which can adjust six parameters in real-time. Finally the efficacy of the DBI system for the medical application is evaluated by a medical doctor who is specialized for endoscopic diagnosis.

## 2. Image enhancement by spectral processing

### 2.1. Spectral estimation from RGB values

The color reproduction characteristics of electronic endoscopes depend on many optical factors with wavelength $\lambda$ (nm) such as spectral radiant distribution of illuminant $E(\lambda)$, spectral sensitivity of CCD $S(\lambda)$, spectral transmittance of color filters $f_i(\lambda),\ i=\{r,g,b\}$, and spectral transmittance of imaging lenses $L(\lambda)$. The output signal $v_i$ at position $(x,y)$ can be calculated as,

$$v_i(x,y)=\int_{vis} E(\lambda)S(\lambda)f_i(\lambda)L(\lambda)r(\lambda,x,y)d\lambda, \qquad i=\{r,g,b\}\,. \tag{1}$$

where $r(\lambda,x,y)$ is a spectral reflectance of the surface. For mathematical convenience, each spectral characteristic with wavelength $\lambda$ is expressed as a vector or a matrix with the discrete form, and further for the sake of simplicity, $(x,y)$ from $v_i$, $r$ are omitted. Equation (1) can be rewritten as follows,

$$\begin{aligned}\mathbf{v} &= \begin{bmatrix} v_r & v_g & v_b \end{bmatrix}^T \\ &= \mathbf{A}\mathbf{r}, \\ \mathbf{r} &= \begin{bmatrix} r(400) & r(405) & \cdots & r(700) \end{bmatrix}^T,\end{aligned} \tag{2}$$

where $T$ denotes a transposition and matrix $\mathbf{A}$ is called system matrix that represents entire characteristics of imaging system. In order to discretize the wavelength in the visible range, we calculate from 400(nm) to 700(nm) with interval of 5(nm). Here the imaging system is assumed to have linear characteristics. In order to handle non-linear characteristics of the imaging system, refer to [16]. The estimation of reflectance spectra $\tilde{\mathbf{r}}$ can be obtained as follows,

$$\tilde{\mathbf{r}} = \mathbf{G}\mathbf{v}, \tag{3}$$

where $\mathbf{G}$ is called a estimation matrix figured out by using an estimation method. In this study we employ the Wiener estimation for $\mathbf{G}$. Wiener estimation method minimizes the overall average of the square error between the original and estimated spectral reflectance [17]. For this method, the estimation matrix $\mathbf{G}$ is given as follows,

$$\mathbf{G} = \mathbf{R}_{rr}\mathbf{A}^T(\mathbf{A}\mathbf{R}_{rr}\mathbf{A}^T + \mathbf{R}_{nn})^{-1}, \tag{4}$$

where $\mathbf{R}_{rr}$ represents the self-correlation matrix of original spectra $\mathbf{r}$, and $\mathbf{R}_{nn}$ represents the self-correlation of noise. Hence Equation 4 can be rewritten as,

$$\mathbf{G} = \mathbf{r}\cdot\mathbf{v}^T(\mathbf{v}\cdot\mathbf{v}^T + \mathbf{R}_{nn})^{-1}, \tag{5}$$

In order to calculate $\mathbf{G}$, it is needed to take number of samples by the CCD. In this study, we use Macbeth Color Checker which has 24 of different color samples and each spectral distribution is first measured by using a spectrophotometer. Thus 24 sets of measured spectral distribution is used for $\mathbf{r}$ in Eq.(5), and 24 sets of $\mathbf{v}$ are given by the output signal of the CCD by taking the Macbeth Color

Checker.

## 2.2. Image enhancement by estimated spectral information

In 2005, Miyake et al. proposed the image enhancement method [14] by assigning three single band images of arbitrary wavelength to R, G, B image planes. For example, by choosing 500nm for R plane, 450nm for G plane, 410nm for B plane from an estimated 61-bands spectral image, a synthesized example is shown in Fig. 1. The edge of the tumor area is clearly emphasized by using this method. This color transformation is just multiplying a $3\times3$ matrix to the pixel values of CCD output $\mathbf{v}=[v_r \quad v_g \quad v_b]^T$ as follows,

$$\begin{aligned}\mathbf{p} &= \mathbf{FG}\cdot\mathbf{v}, \\ &= \mathbf{M}\cdot\mathbf{v},\end{aligned} \tag{6}$$

where $\mathbf{p}$ is the output RGB vector and $\mathbf{F}$ is selection and filtering matrix which converts from 61-band spectral data to RGB data. $\mathbf{M}$ used actually in Figure 1 is

$$\mathbf{M}=\begin{bmatrix} -0.00119 & 0.002346 & 0.001600 \\ 0.004020 & 0.000068 & -0.000970 \\ 0.005152 & -0.001920 & 0.000088 \end{bmatrix}. \tag{7}$$

Since this operation is very simple, it is easy to implement it to the conventional endoscope system additionally as a software post processing in real-time.

[Fig.1 about here]

In the practical diagnosis, medical doctors have to diagnose the hundreds kinds of tumors on the mucous membrane which has different spectral properties. When a tumor has particular reflectance spectra which is clearly different from reflectance spectra of mucous membrane, the conventional method is effective to emphasize the edge. There are, however, many tumors which has quite similar reflectance spectra to the membrane. In order to enhance such slight difference of spectral properties, we propose a new method named dynamic band imaging.

### 2.3. Dynamic Band Imaging (DBI)

Human perception has more sensitivity against temporally changing stimulus than the still stimulus, e.g. small involuntary eye movement. In order to distinguish slight color difference, color-enhanced movies may be more effective than still images. Since endoscopic diagnoses are conventionally performed by evaluating the still images, in this study we generate the color-enhanced movie from the still image based on the spectral processing described before.

In this method, for designing the matrix $\mathbf{F}$ we define three kinds of time-varying parameters such as center wavelength $c_i(t)$ (nm), band width $w_i(t)$ and intensity coefficient $n_i(t)$, where $t$ is the time and $i$ represents color channels, $i = \{r, g, b\}$. This method is namely equivalent to change the transformation matrix $\mathbf{M}$ dynamically, and then we call it dynamic band imaging (DBI).

By using estimated reflectance spectra $\tilde{r}(\lambda)$ calculated with $\mathbf{G}$, output digital values can be synthesized by using the equation of Gaussian distribution as follows,

$$p_i = n_i(t) k_i \sum_{\lambda=\{400,405,\cdots,700\}} \frac{1}{\sqrt{2\pi} w_i(t)} \exp\left( -\frac{(\lambda - c_i(t))^2}{2 w_i(t)^2} \right) \tilde{r}(\lambda)\,. \tag{8}$$

Coefficient $k_i$ is determined to give $(p_r, p_g, p_b) = (255,255,255)$ when the camera takes the perfect reflecting diffuser as follows,

$$k_i \sum_{\lambda=\{400,405,\cdots,700\}} \frac{1}{\sqrt{2\pi} w_i(t)} \exp\left( -\frac{(\lambda - c_i(t))^2}{2 w_i(t)^2} \right) = 255\,. \tag{9}$$

In this method, we have infinite degrees of freedom to define these time-varying functions. In order to analyze the fundamental efficacy of DBI, we prepare two kinds of changing functions of parameters. The first one is

$$
\begin{aligned}
c_i(t) &= \begin{cases} c_i^{low} + 2dt(c_i^{high} - c_i^{low}) & \text{if} \quad 0 \le t < \frac{1}{2d}, \\ c_i^{low} + 2(1-dt)(c_i^{high} - c_i^{low}) & \text{if} \quad \frac{1}{2d} \le t < \frac{1}{d}, \end{cases} \\
w_i(t) &= 10, \\
n_i(t) &= 1,
\end{aligned}
\tag{10}
$$

where $c_i^{low}, c_i^{high}$ (nm) are the lower and higher boundaries of the oscillation of the center wavelength respectively and $d$ (Hz) represents the frequency of the oscillation. Then $c_i(t)$ is the triangular wave function as shown in Fig. 2(a). In this study, we focus on to investigate the efficacy of center wavelength and let band width and intensity coefficient constant. The secondly prepared changing function is as follows,

$$
\begin{aligned}
c_i(t) &= \begin{cases} c_i^{low} & \text{if} \quad 0 \le t < \frac{1}{2d}, \\ c_i^{high} & \text{if} \quad \frac{1}{2d} \le t < \frac{1}{d}, \end{cases} \\
w_i(t) &= 10, \\
n_i(t) &= 1,
\end{aligned}
\tag{11}
$$

This shapes simple square wave shown in Fig. 2(b). Using these ways, the effectiveness of dynamic band imaging can be evaluated in comparison with the still image evaluation.

[Fig.2 about here]

## 3. Experiments

Dynamic band imaging has been proposed based on the hypothesis that color-enhanced movies may be more effective than still images to distinguish slight color difference. Therefore in order to investigate the fundamental effectiveness of DBI, we have conducted a basic experiment by way of subjective evaluations. In this experiment, we have prepared eight example combinations of similar reflectance spectra. Each combination consists of two kinds of reflectance spectra extracted from arbitrary human skin color database. The color differences $\Delta E_{94}$ under D65 illumination between them and all reflectance spectra are shown in Fig. 3. A small square patch which is colored by the first reflectance spectra is placed on a random position over the large square patch colored by the second reflectance spectra as shown in Fig. 4. The efficacy of the image enhancement is evaluated by judging whether the small patch can be found or not.

[Fig.3 about here]

[Fig.4 about here]

These color patches are taken by a camera simulator which has the typical spectral sensitivity $Q_i(\lambda) = S(\lambda) f_i(\lambda) L(\lambda)$ as shown in Fig. 5. By using this camera simulator, we first calculate the estimation matrix $\mathbf{G}$ which gives $\tilde{r}(\lambda)$ from $v_i$ by means of Wiener estimation described in Section 2. Dynamic band imaging described in Eq. (8) is performed with the triangular wave (Eq. (10)) and the square wave (Eq. (11)). For the subjective evaluation, we prepare six kinds of imaging scheme as follows

Case A: Color patches are displayed as is taken by the camera simulator

Case B: DBI with 2Hz triangular waveform using estimated reflectance spectra $\tilde{r}(\lambda)$. This is set as baseline.

Case C: DBI with slower changing speed than case B.

Case D: DBI with smaller amplitude of the wave oscillation than case B.

Case E: DBI with square waveform.

Case F: DBI using original reflectance spectra $r(\lambda)$.

[Fig.5 about here]

Actual DBI parameters used in case B to F are shown in Table 1. For the subjective evaluation, 48 movie patches (eight sets of skins colors times six cases) are displayed on the LCD monitor for five seconds each in random order. Subjects are asked whether they could find the small square patch inside the large square patch or not (Fig. 4). The distinguishable rates of six cases evaluated by eleven subjects (21-30 years old) are shown in Fig. 6. To examine the efficacy of the proposed method, the logistic regression analysis is employed. First we compare the static image (Case A) with DBI (Case B to F) by varying the range of color difference and the results appear in Table 2. We see from Table 2 that significant efficacy (p=0.025<0.05) is obtained in the range of $\Delta E_{94} = (0.623,\ 0.798)$, but not significant in $\Delta E_{94} \leq 0.436$ and $\Delta E_{94} \geq 0.927$. This means that $\Delta E_{94} \geq 0.927$ represents enough large color difference and most of subjects could distinguish two colors in this range, and $\Delta E_{94} \leq 0.436$ is actually too small difference to enhance by DBI. Hence DBI is effective to improve the distinguishable rate of color difference around $\Delta E_{94} = (0.623,\ 0.798)$. Next we examine the difference between parameters of DBI by using the logistic regression analysis as shown in Table 3. p value for each combination is calculated between results of baseline case (B) and each cases (C to F). Table 3(a), which shows results in the range of $\Delta E_{94} = (0.623,\ 0.798)$, actually appears no significant difference, whereas we can see high efficacy (p=0.053) of Case E against Case B in the range of $\Delta E_{94} = (0.266,\ 0.436)$. It is likely that the square waveform has the possibility to emphasize the very small color difference.

[Table.1 about here]

[Fig.6 about here]

[Table.2 about here]

[Table.3 about here]

## 4. Endoscopic diagnosis

As the practical application of DBI, we implement the real-time DBI system for endoscopic diagnosis as shown in Fig. 7. Because DBI has many parameters which need to change simultaneously, it is very difficult task to determine the best change of parameters by using conventional man-machine interface, such as ordinary mouse and keyboard. Therefore we propose to use PHANTOM$^R$ (SensAble technologies) in order to determine the best parameters of DBI, which is an input interface having six degrees of freedom. Six parameters of DBI (center wavelength $c_i(t)$ and intensity $n_i(t)$) are assigned to the $X,Y,Z$ coordinate and roll, yaw, pitch angles of PHANTOM$^R$'s stylus, respectively. Medical doctors can seek the best changing way of the six parameters with displaying the endoscopic image in real-time. Figure 8 shows an example change determined by a medical doctor who is the young specialist for the endoscopic diagnosis with the purpose of enhancing the slight cancer on the mucous membrane of the stomach. The endoscopic image used in this evaluation is shown in Fig. 7. After the evaluation of DBI by the medical doctor, he commented that DBI is a new effective method to enhance the image for medical diagnosis and the interface is very useful to determine many parameters at the same time.

[Fig.7 about here]

[Fig.8 about here]

## 5. Conclusion

In this study, we propose a new image enhancement technique named dynamic band imaging (DBI) for the endoscopic diagnosis. This method is based on the hypothesis that color-enhanced movies may be more effective than still images to distinguish slight color difference. Therefore at first, in order to investigate the fundamental efficacy of DBI, we conducted subjective experiments with six cases of parameters of DBI. From the results of logistic regression analysis, we found that DBI is significantly effective to improve the distinguishable rate of color difference around $\Delta E_{94} = (0.623,\ 0.798)$. Beside that the square waveform has the possibility to emphasize the very small color difference $\Delta E_{94} = (0.266,\ 0.436)$ in comparison with the triangular waveform. Because the parameters variation of DBI can be designed freely, we need to analyze the efficacy by accumulating the fundamental experiments and need to find more effective parameters by evaluating many practical medical images.

In order to determine many time-varying parameters at the same time, we adopted PHANTOM$^{R}$ interface which has six degrees of freedom input. According to the medical doctor who evaluates the DBI system with this interface, it is the effective system for the practical diagnosis. In the future, we need to apply the outcome of fundamental experiments into the medical application.

**Acknowledgments**

We are grateful to Professor Teruo Kozu of Department of Optical Medicine, Chiba University Hospital for giving us valuable advice. This work is supported by Grant-in-Aid for Young Scientists B (19700413)

**References**

[1] S.Shimizu, "Color Enhancement in Colonoscopy May Be Effective for Detection of Superficial

Type Colorectal Tumors," Digestive Endoscopy, 14(s1), pp.S62-S64 (2002)

[2] K.Nakamura, "Development of Real-time Endoscopic Image Processing Technology: Adaptive Index of Hemoglobin Color Enhancement Processing," Digestive Endoscopy, 14(s1), pp.S40-S47 (2002)

[3] K.Kobayashi, M.Igarashi, M.Sada, T.Katsumata and K.Saigenji, "Clinical Significance of Adaptive Index of Hemoglobin Color Enhancement for Endoscopic Diagnosis of Superficial Type Colorectal Tumors," Digestive Endoscopy, 14(s1), pp.S51-S53 (2002)

[4] Y.Toyota, H.Honda, T.Omoya, K.Inayama, M.Suzuki, K.Kubo, M.Nakasono, N.Muguruma, S.Okamura, I.Shimizu, K.Ii and S.Ito, "Usefulness of a Hemoglobin Index Determined by Electronic Endoscopy in the Diagnosis of Helicobacter Pylori Gastritis," Digestive Endoscopy, 14(4), pp.156-162 (2002)

[5] T.Fujii, A.Ono, "Is Adaptive Index of Hemoglobin Color Enhancement Effective in Detecting Small Depressed Type Colorectal Cancers?," Digestive Endoscopy, 14(s1), pp.S58-S61 (2002)

[6] J.Haringsma, G.N.J. Tytgat, H.Yano, H.Iishi, M.Tatsuta, T.Ogihara, H.Watanabe, N.Sato, N.Marcon, B.C. Wilson and R.W. Cline, "Autofluorescence Endoscopy: Feasibility of Detection of GI Neoplasms Unapparent to White Light Endoscopy with an Evolving Technology," Gastrointestinal Endoscopy, 53(6), pp.642-650 (2001)

[7] N.Uedo, H.Iishi, M.Tatsuta, T.Yamada, H.Ogiyama, K.Imanaka, N.Sugimoto, K.Higashino, R.Ishihara, H.Narahara and S.Ishiguro, "A Novel Videoendoscopy System by Using Autofluorescence and Reflectance Imaging for Diagnosis of Esophagogastric Cancers,"

Gastrointestinal Endoscopy, 62(4), pp.521-528 (2005)

[8] N.Nakaniwa, A,Namihisa, T.Ogihara, A.Ohkawa, S.Abe, A.Nagahara, O.Kobayashi, J.Sasaki and N.Sato, "Newly Developed Autofluorescence Imaging Videoscope System for the Detection of Colonic Neoplasms," Digestive Endoscopy, 17(3), pp.235-240 (2005)

[9] K.Gono, M.Yamaguchi, N.Ohyama, "Improvement of Image Quality of the Electroendoscope by Narrowing Spectral Shapes of Observation Light," Proc. International Congress of Imaging Science. 5, pp.399-400 (2002)

[10] K.Gono, K.Yamazaki, N.Doguchi, T.Nonami, T.Obi, M.Yamaguchi, N.Ohyama, H.Machida, Y.Sano, S.Yoshida, Y.Hamamoto and T.Endo, "Endoscopic Observation of Tissue by Narrowband Illumination", OPTICAL REVIEW, 10(4), pp.211-215 (2003)

[11] K.Gono, T.Obi, M.Yamaguchi, N.Ohyama, H.Machida, Y.Sano, S.Yoshida, Y.Hamamoto, T.Endo, "Appearance of Enhanced Tissue Features in Narrow-Band Endoscopic Imaging," Journal of Biomedical Optics, 9(3), pp.568-577 (2004)

[12] T.Yoshida, H.Inoue, S.Usui, H.Satodate, N.Fukami and S.Kudo, "Narrow-band Imaging System with Magnifying Endoscopy for Superficial Esophageal Lesions," Gastrointestinal Endoscopy, 59(2), pp.288-295 (2004)

[13] M.Muto, T.Ugumori, Y.Sano, A.Ohtsu and S.Yoshida, "Narrow-band Imaging Combined with Magnified Endoscopy for Cancer at the Head and Neck Region," Digestive Endoscopy, 17(s1), pp.S23-S24 (2005)

[14] Y.Miyake, T.Kouzu, S.Takeuchi, T.Nakaguchi, N.Tsumuta and S.Yamataka, "Development of New

Electronic Endoscopes Using the Spectral Images of an Internal Organ", Proc. the 13th Color Imaging Conference (CIC13), pp.261-263 (2005)

[15] Y.Miyake, T.Sekiya, S.Kubo and T.Hara: "A New Spectrophotometer for Measuring the Spectral Reflectance of Gastric Mucous Membrane", J. Photographic Science, 37, pp.134-138 (1989).

[16] C.Munzenmayer, D.Paulus, T.Wittenberg, "A Spectral Color Correction Framework for Medical Applications," IEEE Trans. on Biomedical Engineering, 53(2) pp.254-265 (2006)

[17] H.Haneishi, T.Hasegawa, A.Hosoi, Y.Yokoyama, N.Tsumura, and Y.Miyake, “System design for accurately estimating the spectral reflectance of art paintings,” Applied Optics, 39, pp.6621-6632 (2000)

## List of Figures

List of Tables

Table 1

DBI parameters of test case B to F.

| case | waveform | freq. | $c_r^{low}$ | $c_r^{high}$ | $c_g^{low}$ | $c_g^{high}$ | $c_b^{low}$ | $c_b^{high}$ |
|---|---|---|---|---|---|---|---|---|
| B | **triangular** | **2 Hz** | **600** | **680** | **500** | **580** | **420** | **500** |
| C | triangular | **1 Hz** | 600 | 680 | 500 | 580 | 420 | 500 |
| D | triangular | 2 Hz | **620** | **660** | **520** | **560** | **440** | **480** |
| E | **square** | 2 Hz | 600 | 680 | 500 | 580 | 420 | 500 |
| F | triangular | 2 Hz | 600 | 680 | 500 | 580 | 420 | 500 |

Table 2

Results of logistic regression analysis by varying the range of color difference. ($p < 0.05$) represents significant difference between results of static image (Case A) and DBI (Cases B to F). We obtain significant efficacy of DBI in the range of $\Delta E_{94} = (0.623,\ 0.798)$.

| | | |
|---|---|---|
| Range 1 | dE94=(0.266, 2.055) | p = 0.210 > 0.05 |
| Range 2 | dE94=(0.266, 0.934) | p = 0.242 > 0.05 |
| Range 3 | dE94=(0.266, 0.798) | p = 0.051 > 0.05 |
| Range 4 | dE94=(0.266, 0.436) | p = 0.479 > 0.05 |
| Range 5 | dE94=(0.623, 0.798) | p = 0.025 < 0.05 (*) |
| Range 6 | dE94=(0.623, 0.934) | p = 0.328 > 0.05 |
| Range 7 | dE94=(0.927, 0.934) | p = 0.355 > 0.05 |

Table 3

Results of logistic regression analysis between results of baseline case (B) and each cases (C to F) in the range of (a) $\Delta E_{94} = (0.623,\ 0.798)$, and (b) $\Delta E_{94} = (0.266,\ 0.436)$. It actually shows no significant difference in the range of $\Delta E_{94} = (0.623,\ 0.798)$, whereas Case E shows high difference (p=0.053) in the range of $\Delta E_{94} = (0.266,\ 0.436)$.

(a) $\Delta E_{94} = (0.623,\ 0.798)$

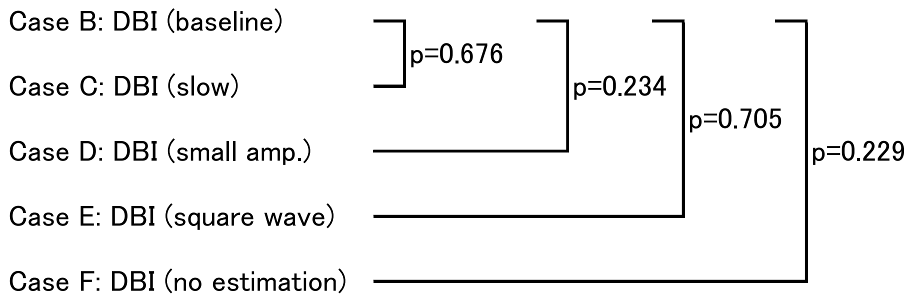


(b) $\Delta E_{94} = (0.266,\ 0.436)$

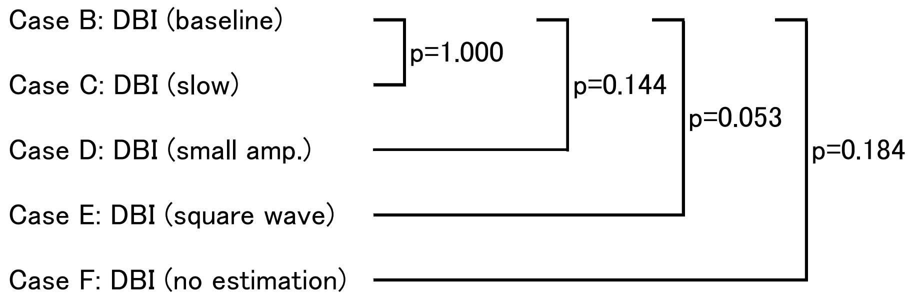

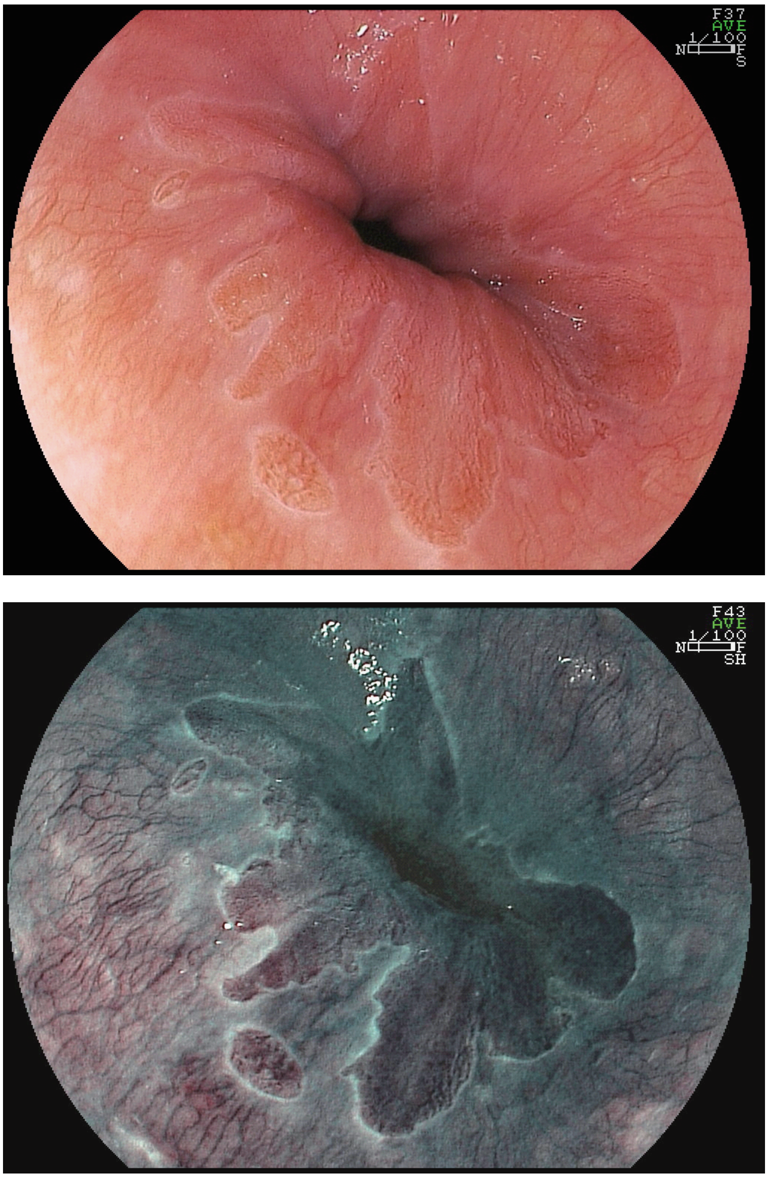

(a)
original

(b)
R: 500nm
G: 450nm
B: 410nm

Fig. 1. (a) Ordinary endoscopic image, (b) Synthesized image by assigning spectral images at 500nm, 450nm and 410nm to R,G,B planes respectively.

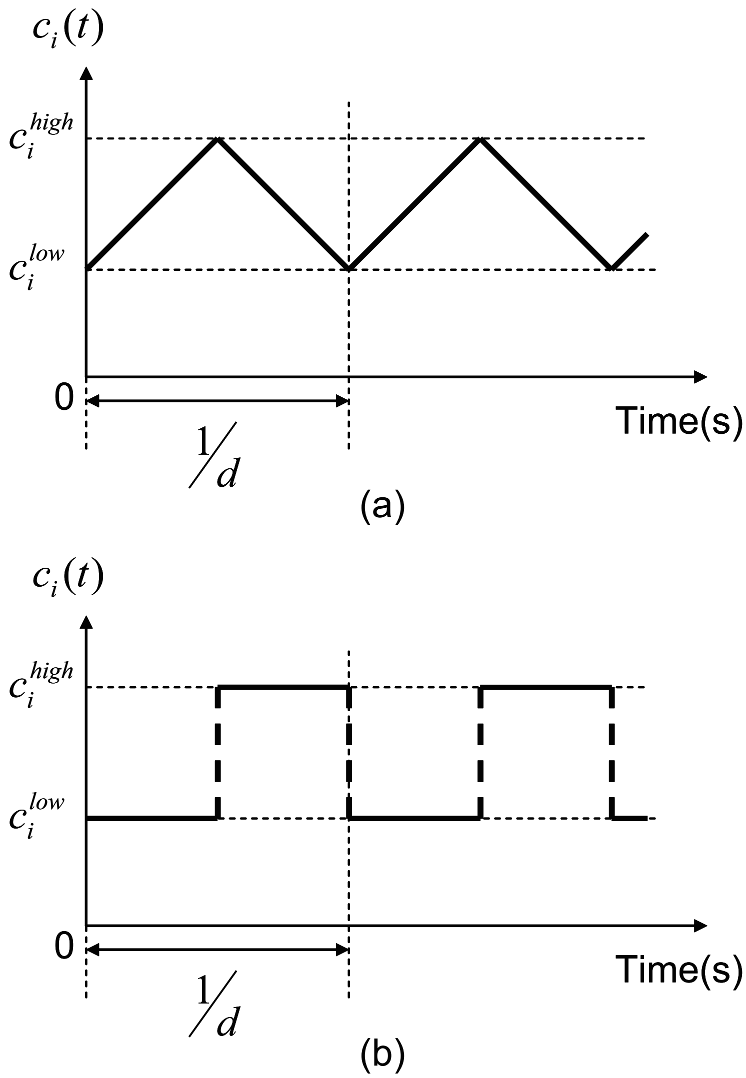


Fig. 2. Temporally changing functions of the center wavelength $c_i(t)$ (a) triangular waveform, (b) square waveform.

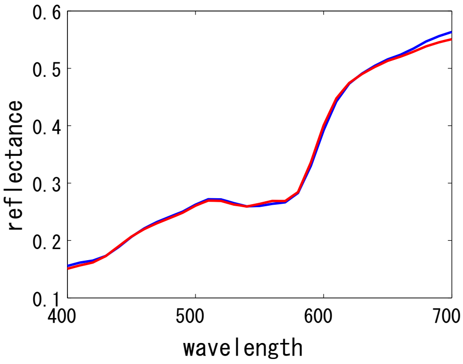


SC1 $\Delta E_{94} = 0.2659$

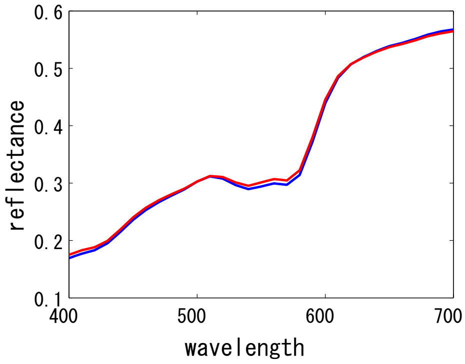


SC2 $\Delta E_{94} = 0.4356$

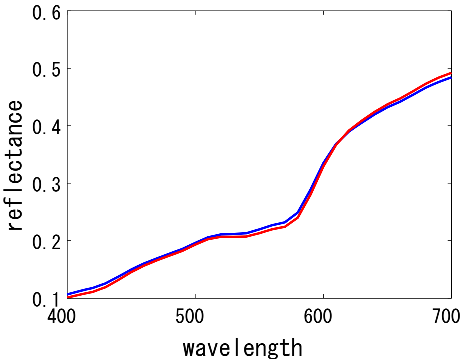


SC3 $\Delta E_{94} = 0.6231$

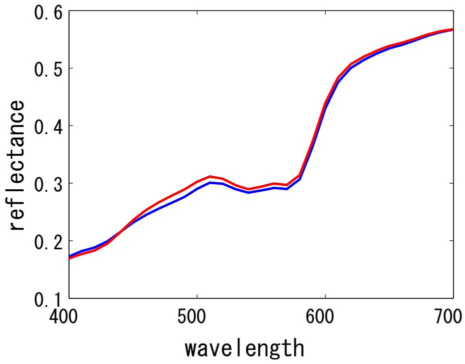


SC4 $\Delta E_{94} = 0.7981$

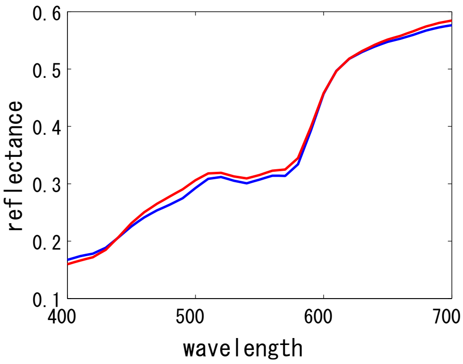


SC5 $\Delta E_{94} = 0.9266$

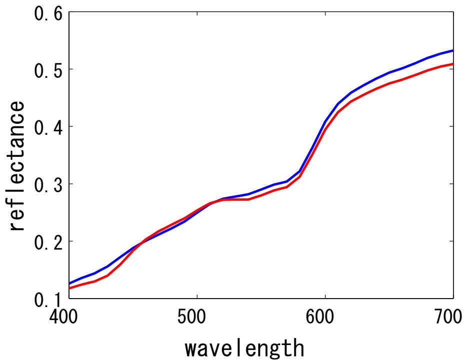


SC6 $\Delta E_{94} = 0.9334$

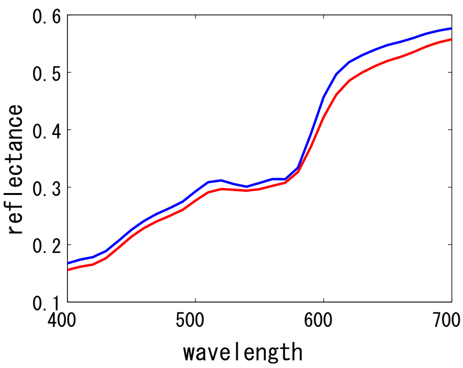


SC7 $\Delta E_{94} = 1.5048$

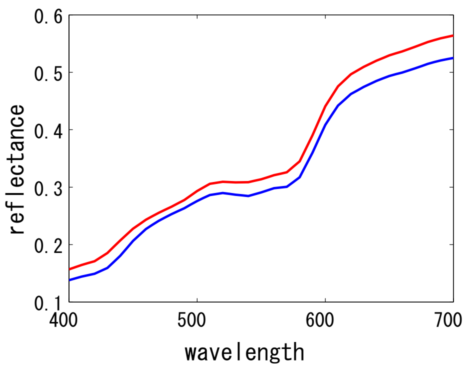


SC8 $\Delta E_{94} = 2.0547$

Fig. 3. Eight sets of reflectance spectra used in the subjective experiment. Each color difference $\Delta E_{94}$ is calculated under D65 illumination.

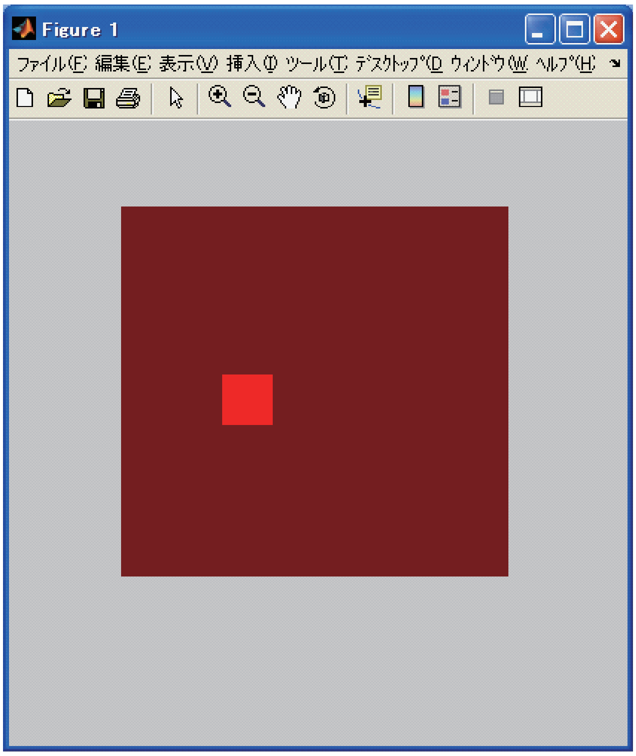


Fig. 4. Display image of the subjective experiment. A small color patch is placed on the large color patch.

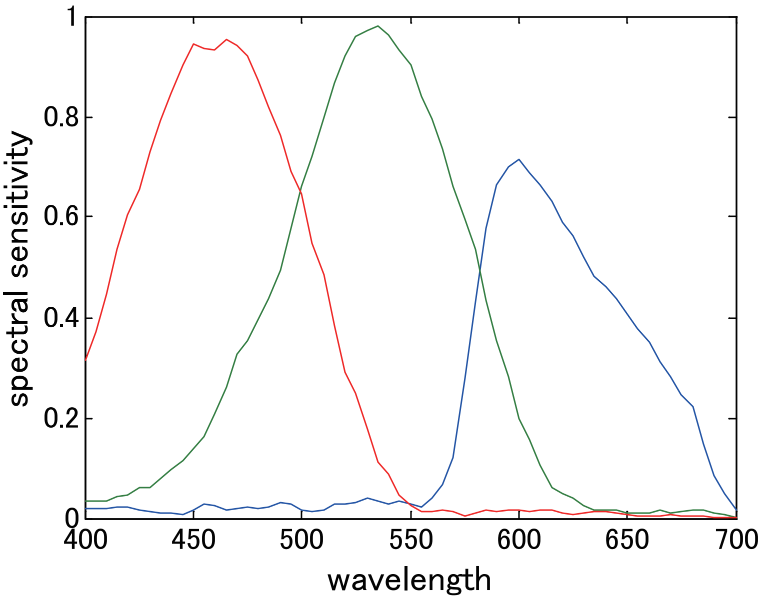


Fig. 5. Spectral sensitivity $Q_i(\lambda) = S(\lambda) f_i(\lambda) L(\lambda)$ of the camera simulator.

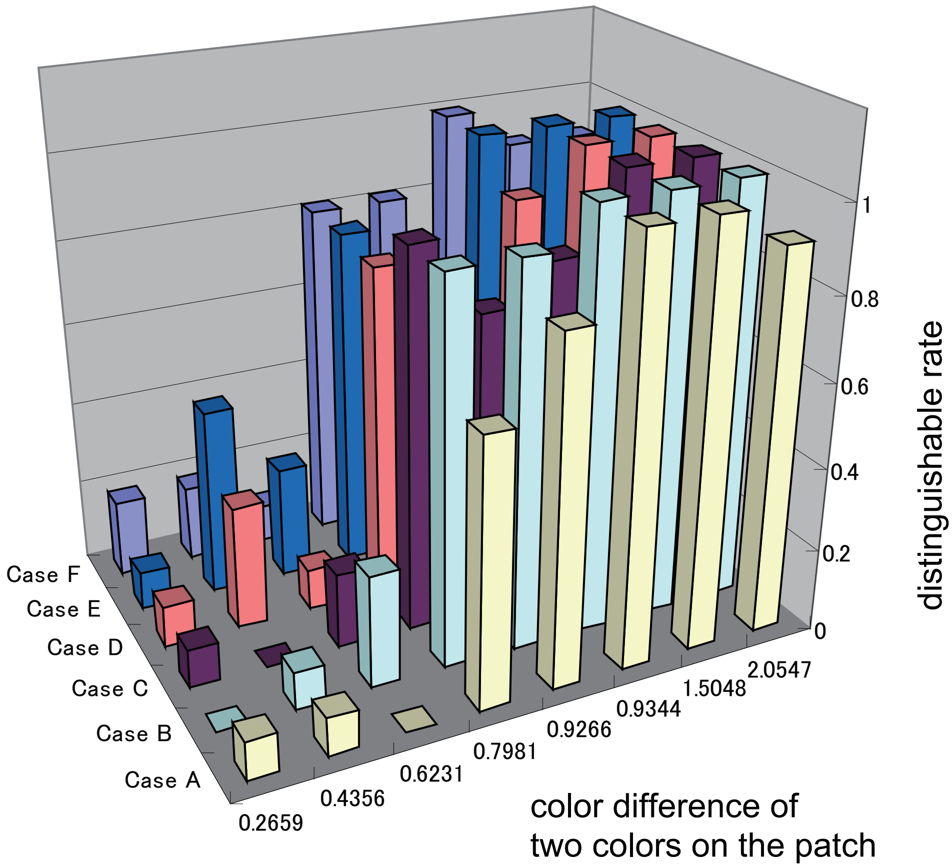


Fig. 6. Results of subjective evaluation. Distinguishable rates of each case are shown.

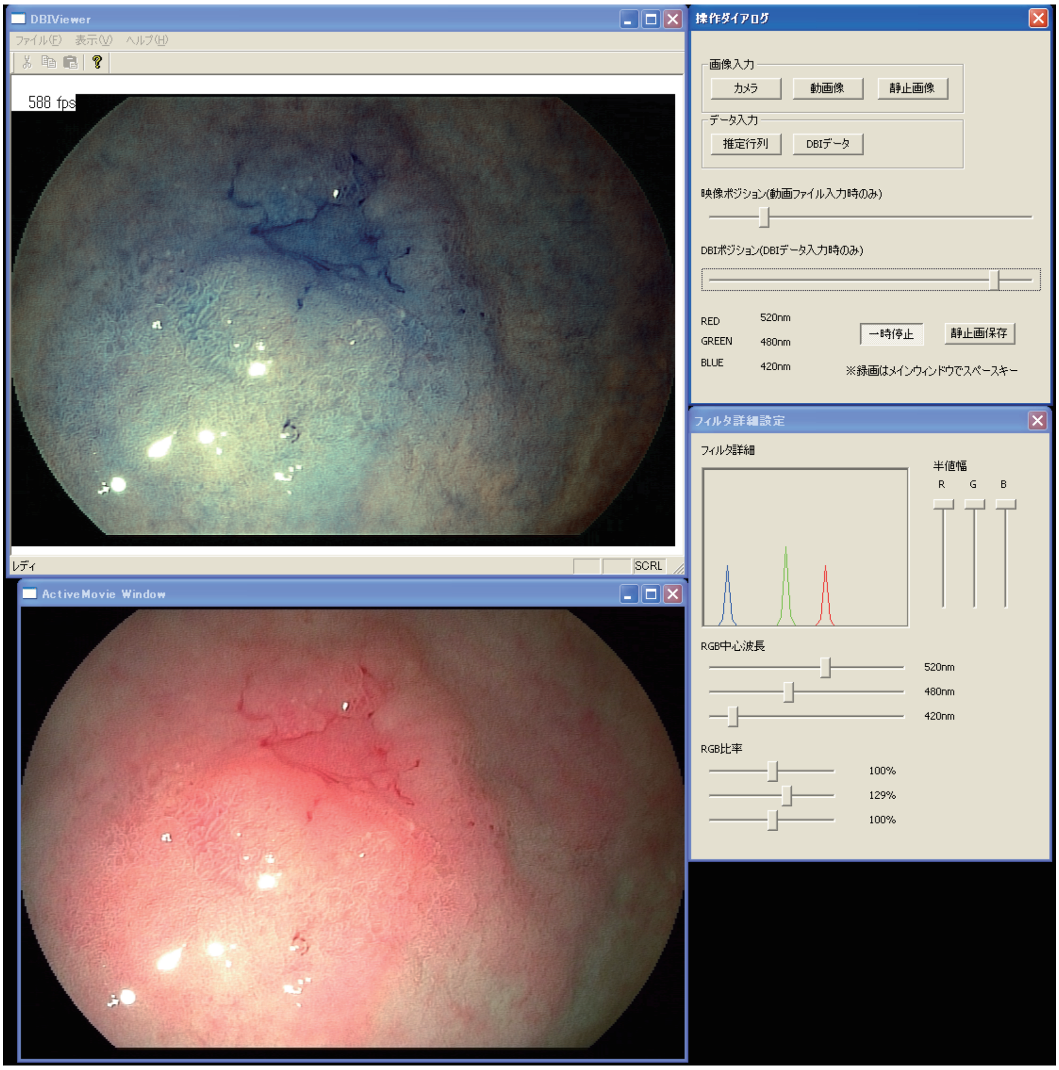


Fig. 7. DBI application for endoscopic diagnosis.

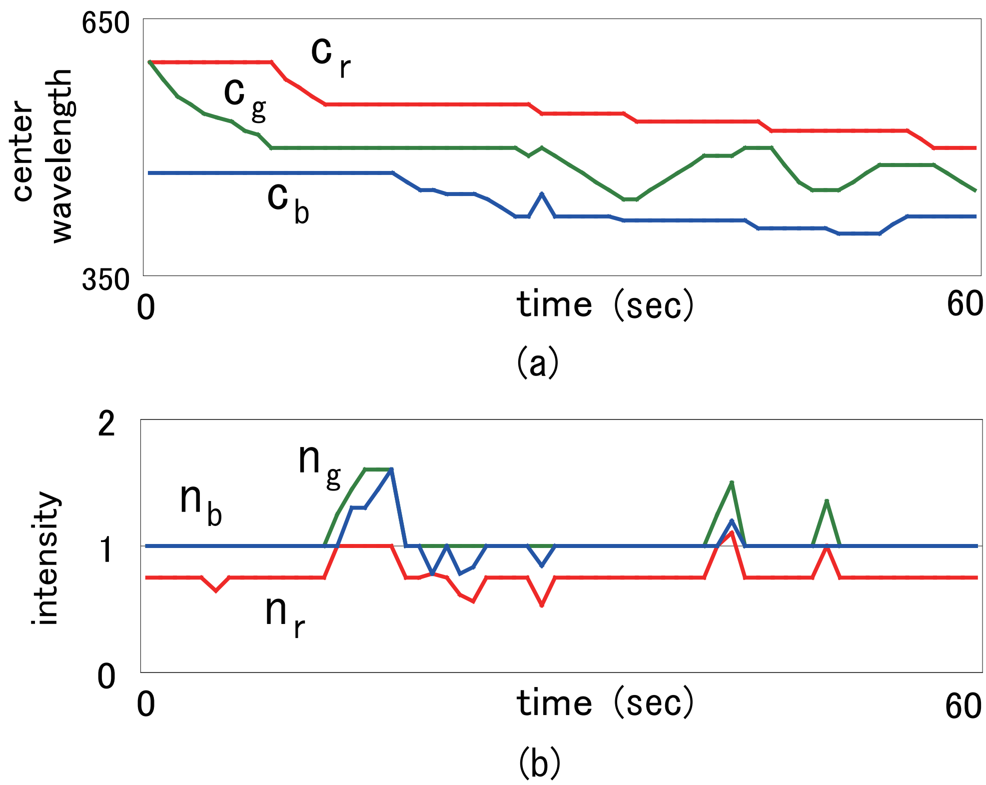


Fig. 8. An example change of (a) center wavelength $c_i(t)$ and (b) intensity $n_i(t)$ determined by a medical doctor using PHANTOM.